Theoretical study of Quark-Gluon-Plasma with jet quenching

Subrata Pal

Department of Nuclear and Atomic Physics,
Tata Institute of Fundamental Research,
Homi Bhabha Road, Mumbai 400005, India

Heavy ion collisions at the Relativistic Heavy Ion Collider (RHIC) and recently at the Large Hadron Collider (LHC) have revealed a new state of matter comprising of strongly coupled quark-gluon plasma (sQGP). Primary evidence of this is provided by the observed suppression of high transverse momenta hadron spectra in central heavy ion collisions relative to both peripheral and nucleon-nucleon collision. In the talk, I will address hadron production and their suppression at RHIC/BNL and in particular at LHC/CERN within a multiphase transport (AMPT) model whose initial conditions are obtained from the recently updated HIJING 2.0 model. The sensitivity of the charged hadron multiplicity $dN_{\rm ch}/d\eta$ on final-state partonic and hadronic scatterings will be discussed. I will show that the observed centrality dependence of $dN_{\rm ch}/d\eta$ can be used to constrain the largely uncertain nuclear modifications of the gluon distribution function. With such a constrained parton shadowing, charged hadron and neutral pion production over a wide transverse momenta range will be presented in AMPT. Relative to nucleon-nucleon collision, the observed suppression of particle yield in central heavy ion collisions will be demonstrated as essentially due to parton energy loss in the hot and dense QGP. While the model calculation of the suppression is consistent with measurements in Au+Au collisions at $\sqrt{s_{NN}} = 0.2$ TeV at RHIC, the suppression is distinctly overpredicted in Pb+Pb collisions at the LHC energy of $\sqrt{s_{NN}} = 2.76$ TeV. The implications and new challenges to understand the unexpectedly transparent strongly coupled QGP formed at LHC will be discussed.

1. Introduction

A novel state of matter, the strongly interacting quark gluon plasma (sQGP) [1], has been created in Au+Au reactions at the Relativistic Heavy Ion Collider (RHIC) [2–5] and recently at the Large hadron Collider (LHC) [6, 7]. Evidence of this is provided by the hydrodynamic model analysis of elliptic (anisotropic) flow data that requires an extremely small shear viscosity to entropy density ratio [8, 9] and primarily from the observed suppression at high transverse momentum, p_T, of single hadron spectra as well as away side hadrons in the back-to-back correlation [10, 11] in central heavy ion collisions relative to the spectra from baseline nucleon-nucleon collisions and peripheral heavy ion collisions. The suppression has been firmly established as due to energy loss by hard partons propagating in the plasma dominantly by radiative gluon emission, referred to as jet quenching [12, 13]. Since the parton scatterings occur at the early stage of the evolution in nuclear collisions, study of energy loss can probe the sQGP phase of the matter. In fact, the magnitude of energy loss is predicted to be strongly dependent on the parton density of the medium which reappears as soft hadrons [13, 14].

In addition to the final state parton energy loss, the jet quenching at moderate and high p_T is also influenced by initial spatial distribution of partons, collective flow, and to the unknown nuclear shadowing of the parton distribution. As the matter created in Pb+Pb collisions at $\sqrt{s_{NN}} = 2.76$ TeV is at about twice the density and probes parton distribution at a smaller momentum fraction x than at RHIC, analysis of the recent data for bulk hadron production [15, 16] and high-p_T hadron sup-

pression at LHC [17, 18] may provide crucial insight into the nuclear medium effects of parton shadowing and energy loss in the hot and dense QCD matter.

While perturbative quantum chromodynamics (pQCD) can address only hard scatterings, formation of strongly coupled near perfect fluid as well as abundant soft particle production suggest a highly nonperturbative physics which is not yet well-established within QCD. Consequently models based on (non-)ideal hydrodynamics [8, 9, 19], transport calculations [20–22] have been developed. It was recently demonstrated in the HIJING 2.0 model [23] that the larger uncertainties of the shadowing effects at RHIC [24] can be constrained from comparison of the measured charged particle density at midrapidity for the most central Pb+Pb collision at LHC. On the other hand, collision centrality dependence of bulk hadron observables should reflect the relative contribution to particle production from hard and soft processes. Thus a precise estimate of nuclear shadowing and detailed study of medium effects on particle production from soft to the hard scattering regime relies on systematic inclusion of various stages of dynamical evolution of matter.

In the talk we shall discuss bulk charged particle production and jet suppression within A MultiPhase Transport (AMPT) model [21] modified to include the modern parton distribution functions and energy dependence in the minijet and soft particle production. In absence of control d+Pb data essential to calibrate the nuclear shadowing of initial jet spectra, we shall use the centrality dependence of charged particle pseudorapidity density, $dN_{\rm ch}/d\eta$, of the ALICE data in Pb+Pb collisions to provide a more stringent constraint on the gluon shadowing parameter s_g which will be then employed to investigate jet suppression. In the sec 2 the AMPT model updated with the new initial conditions will be presented. In sec 3 the model calculations of charged particle production and their suppression at the RHIC and LHC energies are confronted with the data. Finally in sec 4 the summary and conclusions are presented.

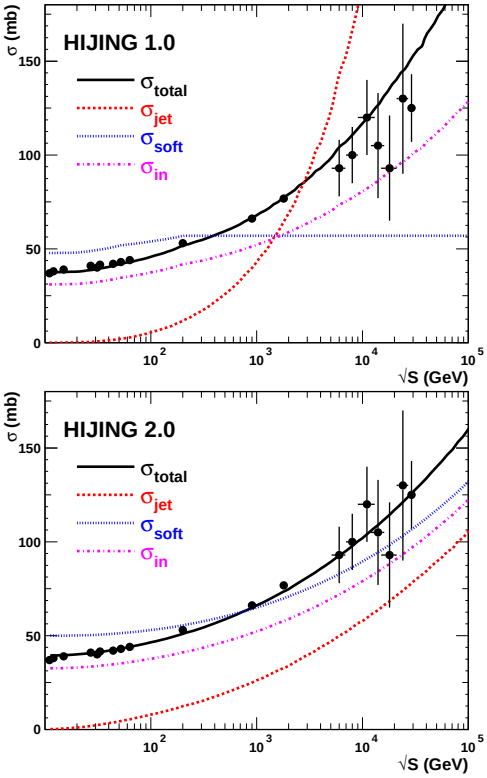

FIG. 1: Experimental values for total, soft and jet production cross sections in $p+p$ and $p+\bar{p}$ collisions at various collision energies as compared to the HIJING 1.0 (top panel) and HIJING 2.0 (bottom panel) models [23].

2. The AMPT model

A MultiPhase Transport (AMPT) model [21] which combines the initial particle distribution from HIJING model [25] with subsequent parton cascade via ZPC model and final hadron transport via ART allows a systematic study of hadron production and jet quenching. In the two-component HIJING model [25] for hadron production, nucleon-nucleon collision with transverse momentum p_T transfer larger than a cut-off p_0 leads to jet production calculable by collinearly factorized pQCD model. Soft interactions with $p_T < p_0$ is characterized by an effective cross section $\sigma_{\rm soft}$. In the HIJING 2.0 model [23] the Duke-Owens parametrization [26] of the parton distribution functions has been updated with the mod-

ern Glück-Reya-Vogt (GRV) parametrization [27]. Since the gluon distribution at small momentum fraction x is much larger in GRV, instead of a fixed value for $p_0 = 2$ GeV/c and $\sigma_{\rm soft} = 57$ mb (as used in HIJING 1.0), an energy dependent cut-off for $p_0(\sqrt{s})$ and $\sigma_{\rm soft}(\sqrt{s})$ is used to fit experimental data on total and inelastic cross sections and hadron rapidity density in $p+p/\bar{p}$ collisions [23]. Fig. 1 illustrates the total and inelastic jet production cross sections in $p + p/\bar{p}$ collisions calculated in the HIJING 1.0 and 2.0 and compared to the experimental data [23]. Energy dependence in $p_0(\sqrt{s})$ and $\sigma_{\rm soft}(\sqrt{s})$ result in smaller total cross section $\sigma_{\rm total}$ and enforces much smaller jet production cross section $\sigma_{\rm jet}$ in HIJING 2.0 model.

For the nuclear parton distribution function (PDF), HIJING employs the function form

$$f_a^A(x,Q^2) = A\, R_a^A(x,Q^2)\, f_a^N(x,Q^2) \qquad (1)$$

where the PDF in a nucleon is f_a^N. The nuclear modification factor of quarks and gluons ($a \equiv q, g$) in HIJING 2.0 parametrization are [23]

$$\begin{aligned} R_q^A(x,b) &= 1 + 1.2\ln^{1/6}\!A\,(x^3 - 1.2x^2 + 0.21x) \\ &\quad - s_q(b)\,(A^{1/3}-1)^{0.6}\,(1 - 3.5x^{0.5}) \\ &\quad \times \exp(-x^2/0.01), \\ R_g^A(x,b) &= 1 + 1.2\ln^{1/6}\!A\,(x^3 - 1.2x^2 + 0.21x) \\ &\quad - s_g(b)\,(A^{1/3}-1)^{0.6}\,(1 - 1.5x^{0.35}) \\ &\quad \times \exp(-x^2/0.004). \end{aligned} \qquad (2)$$

The impact parameter dependence of shadowing is taken as $s_a(b) = (5s_a/3)(1-b^2/R_a^2)$ that prohibits rapid rise of particle production with increasing centrality. Here $R_A \sim A^{1/3}$ is the nuclear size and $s_q = 0.1$ is fixed by data from deep inelastic scatterings.

From comparison to the centrality dependence of charged particle pseudorapidity density per participant pair of nucleons, $(dN_{\rm ch}/d\eta)/(\langle N_{\rm part}\rangle/2)$ in Au+Au collisions at $\sqrt{s_{NN}} = 0.2$ TeV, the gluon shadowing parameter in HIJING 2.0 model has been constrained to $s_g = 0.17 - 0.22$. Whereas a stronger constraint of $s_g = 0.20 - 0.23$ has been obtained from the reproduction of $dN_{\rm ch}/d\eta$ ALICE data for the most central (head-on) Pb+Pb collisions at $\sqrt{s_{NN}} = 2.76$ TeV. Albeit the HIJING ignores the final state interaction of particles and such an estimate of s_g is entirely from initial state effects. We shall show the influence of final state parton energy loss [12–14] as well as hadronic rescatterings modify considerably the $dN_{\rm ch}/d\eta$ yield and thereby the magnitude of the initial state nuclear shadowing s_g for gluon distribution. In the present study we shall use the string melting version of the AMPT where the hadrons from HIJING 2.0 are converted to their valence (anti)quarks and parton recombination is employed for hadronization. The coalescence of dominant soft partons and also relatively large number of hard jets produced at LHC will thus contribute to the final charged hadron spectrum. In the Lund string fragmentation function $f(z) \propto z^{-1}(1-z)^a \exp(-bm_T^2/z)$, where z is the light-cone momentum fraction of the generated hadrons with transverse mass m_T, we employ the default HIJING values of $a = 0.5$ and $b = 0.9$ GeV^{-2}. Further the strong coupling constant is taken as $\alpha_s = 0.3$ and screening mass $\mu = 3.2264$ fm^{-1} [28] that correspond to parton-parton elastic cross section of $\sigma \approx 1.5$ mb in the parton cascade.

3. Results and discussions

Figure 2 shows the pseudorapidity distribution of charged hadrons in the 5% most central collision in the AMPT model in Au+Au at $\sqrt{s_{NN}} = 0.2$ TeV and Pb+Pb at $\sqrt{s_{NN}} = 2.76$ TeV. The results are with gluon shadowing parameter of $s_g = 0.15$ (at RHIC) and $s_g = 0.17$ (at LHC) that are found to be in good agreement with the measured $dN_{\rm ch}/d\eta$ distribution from BRAHMS [2, 29] at $\sqrt{s_{NN}} = 0.2$ TeV, and the $dN_{\rm ch}/d\eta\,(|\eta| < 0.5) = 1601 \pm 60$ from ALICE [15] at $\sqrt{s_{NN}} = 2.76$ TeV. In absence of final state partonic and hadronic scatterings, which is basically the HIJING 2.0 model predicts $dN_{\rm ch}/d\eta(|\eta| < 0.5) = 706 \pm 5$ and 1775 ± 3 at RHIC and LHC, respectively. In subsequent parton cascade (i.e. HIJING plus ZPC), energy dissipa-

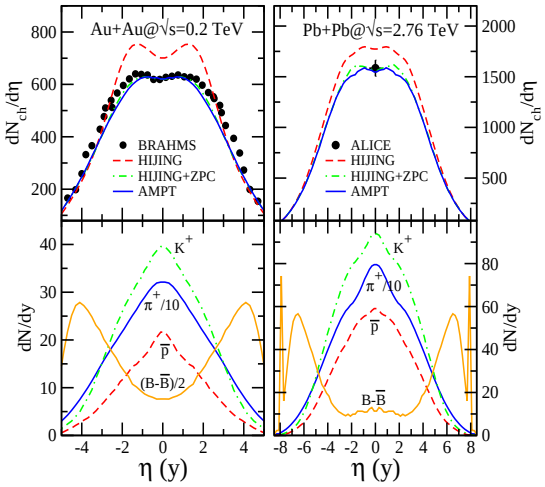

FIG. 2: Top panels: Pseudorapidity distribution for charged hadrons in Au+Au collision at RHIC energy of $\sqrt{s_{NN}}$ = 0.2 TeV and in Pb+Pb collision at LHC energy of $\sqrt{s_{NN}}$ = 2.76 TeV for $(0-5\%)$ centrality. The AMPT model predictions are without any final state interactions as in HIJING (dashed line); with parton transport i.e. HIJING+ZPC (dashed-dotted line), and with further hadron transport as in AMPT (solid line). The solid circles are the measured values from the BRAHMS at RHIC [29] and ALICE at LHC [15]. Bottom panels: The rapidity distribution from AMPT for K^+, π^+, $\bar{p}$ and net baryons, $B-\bar{B}$, at the RHIC and LHC energies.

tion and redistribution into the transverse flow via partonic scattering lead to a reduction of charged particle multiplicity by surprisingly a similar amount of $\sim 15\%$ at both RHIC and LHC. Though the partonic density at LHC is about twice than at RHIC, this nearly equal suppression of yield after parton cascade reflects the interplay between hard and soft processes via a delicate balance between collective flow, gluon shadowing and jet multiplicity all of these are larger at LHC than at RHIC. Finally, subsequent hadronic scatterings (dubbed as AMPT) from the less dense phase leads to a smaller decrease of particle multiplicity. Fig. 2 further shows that final state scatterings essentially smoothen out the dip at $\eta = 0$ (due to Jacobian) in HIJING to a nearly flat $dN_{\rm ch}/d\eta$ distribution around mid-rapidity. Such a weak pseudorapidity-dependence in $dN_{\rm ch}/d\eta$ at $\eta \leq 2$ has also been observed in both the BRAHMS [29] and CMS data [7, 16].

The rapidity distribution of pions, kaons, antiprotons and net baryons are displayed in Fig. 2 at $\sqrt{s_{NN}}$ = 0.2 and 2.76 TeV. With more than an order of magnitude increase in energy at LHC, the rapidity distribution of the produced hadrons becomes wider by $\sim 55\%$ and thereby $dN_{\rm ch}/d\eta$ at midrapidity increases by ~ 2.4 compared to the top RHIC energy. While the net-baryon density is found to decrease by $\sim 35\%$ from $\sqrt{s_{NN}}$ = 0.2 TeV to 2.76 TeV, the antibaryon to baryon ratio at these RHIC (LHC) energies are found to be $\bar{p}/p = 0.70(0.82)$, $\bar{\Lambda}/\Lambda = 0.75(0.85)$, $\bar{\Xi}/\Xi = 0.83(0.89)$ and $\bar{\Omega}/\Omega = 0.89(0.95)$. The yield ratios from the AMPT at RHIC are consistent with the measured values [2–5] within the systematic errors. Enhanced meson production and slight decrease in the strangeness density at LHC result in the ratios at midrapidity of $p/\pi^+ = 0.091$ (0.088) and $K^+/\pi^+ = 0.17$ (0.15) at the RHIC (LHC) energies considered here.

In Fig. 3 we present the charged particle pseudorapidity density per participant pair, $(dN_{\rm ch}/d\eta)/(\langle N_{\rm part}\rangle/2)$, as a function of centrality of collision characterized by average number of participating nucleons $\langle N_{\rm part}\rangle$. The AMPT calculation are for Au+Au collisions at $\sqrt{s_{NN}}$ = 0.2 TeV with a range of gluon shadowing parameter $s_g = 0.10 - 0.17$ and for Pb+Pb at $\sqrt{s_{NN}}$ = 2.76 TeV with $s_g = 0.16 - 0.17$. With this choice of the gluon shadowing parameter, the centrality dependence of charged particle multiplicity agrees well within the experimental uncertainty seen in the PHENIX [30] and BRAHMS data [29] at RHIC. Due to abundant jet and minijet production at LHC, the ALICE multiplicity data for Pb+Pb collision is quite sensitive to nuclear distortions at small x and provides a much stringent constraint on the gluon shadowing of $s_g \simeq 0.17$. It may be mentioned that the estimated values of s_g in AMPT are consistently smaller than in HIJING 2.0 model [23] which underscores the importance of fi-

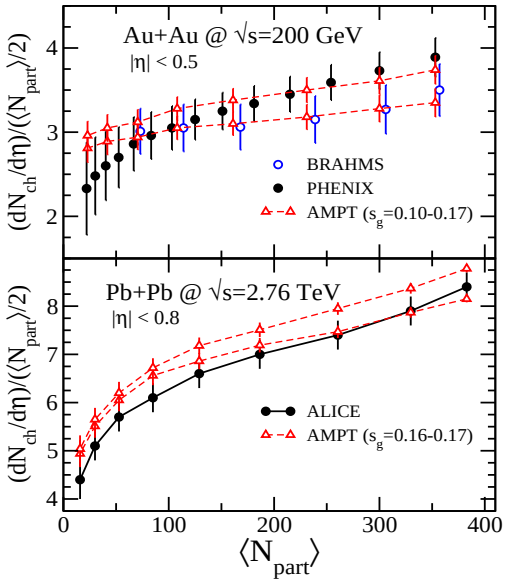

FIG. 3: Charged hadron multiplicity density $dN_{\rm ch}/d\eta$ at mid-rapidity per participant nucleon pair as a function of average number of participants $\langle N_{\rm part}\rangle$. The results are from AMPT calculations (triangles) obtained with gluon shadowing parameter $s_g = 0.10 - 0.17$ in Au+Au collision at $\sqrt{s_{NN}} = 0.2$ TeV (top panel) and with $s_g = 0.16 - 0.17$ in Pb+Pb collision at $\sqrt{s_{NN}} = 2.76$ TeV (bottom panel) as compared with the data (circles) from BRAHMS [29] and PHENIX [30] at RHIC and ALICE [15] at LHC.

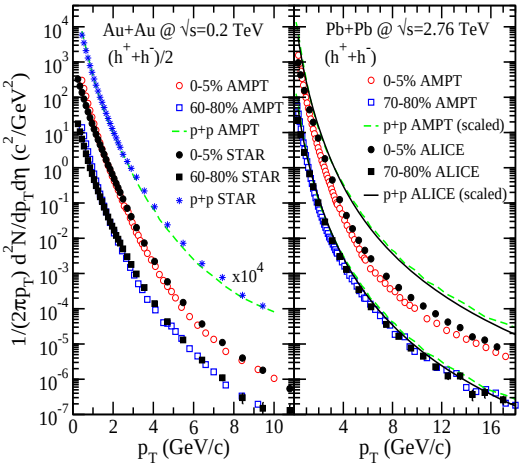

FIG. 4: Invariant hadron production spectrum in $p+p$ and Au+Au collision at $\sqrt{s_{NN}} = 0.2$ TeV (left panel) and in $p+p$ and Pb+Pb collision at $\sqrt{s_{NN}} = 2.76$ TeV (right panel). The results are from AMPT calculations in p+p (dashed lines) and heavy ion $(A+A)$ (open symbols) collisions with gluon shadowing parameter $s_g = 0.15$ (0.17) at RHIC (LHC). The measured spectrum are for Au+Au (solid symbols) and $p+p$ non-single-diffractive interaction (star) by STAR [10] at RHIC and for Pb+Pb (solid symbols) by ALICE [17] at LHC. The $p+p$ reference spectrum at $\sqrt{s_{NN}} = 2.76$ TeV (solid lines) is the ALICE interpolation normalized to LO pQCD which is shown as scaled by average number of binary collisions, $\langle N_{\rm coll}\rangle$, corresponding to the centrality classes.

nal state interactions in precise estimation of the nuclear shadowing of partons that in turn should also influence the hard observables.

The study of bulk hadron production when coupled with that for hadron spectra provide crucial information of the parton-medium interactions where high-p_T partons suffer energy loss that are transported to produce soft hadrons. To quantify such a suppression of hadrons at high p_T due to medium effects in heavy ion collisions, the nuclear modification factor

$$R_{AA}(p_T) = \frac{d^2N^{AA}/d\eta\, dp_T}{\langle N_{\rm coll}\rangle\ d^2N^{pp}/d\eta\, dp_T} \qquad (3)$$

is used which is the ratio of particle yield in heavy ions $(A+A)$ to that in $p+p$ reference spectra, scaled by the total number of binary nucleon-nucleon (NN) collisions $\langle N_{\rm coll}\rangle = \langle T_{AA}\rangle \sigma^{NN}_{\rm inel}$. In absence of initial and final state nuclear medium effects $R_{AA}(p_T) = 1$ by construction. The nuclear thickness function $\langle T_{AA}\rangle$ and the inelastic NN cross section $\sigma^{NN}_{\rm inel}$ are calculated within the HIJING 2.0 model that uses Glauber Monte Carlo simulation for distribution of initial nucleons with a Woods-Saxon nuclear density. The energy dependent soft interaction cross section $\sigma_{\rm soft}(\sqrt{s})$ in HIJING 2.0 enforces $\sigma^{NN}_{\rm inel}$ to be about 42 and 64 mb at $\sqrt{s_{NN}} = 0.2$ and 2.76 TeV, respectively. However, at low p_T regime dominated by soft particle production, the scaling by the number of nucleons suffering at least one inelastic collision, i.e $N_{\rm part}$, is more appropriate.

Figure 4 shows the inclusive charged hadron p_T spectra at midrapidity in the AMPT for $p+p$ collisions and for central $(0-5\%)$ and peripheral Au+Au collisions at $\sqrt{s_{NN}} = 200$ GeV (left panel) and in Pb+Pb collisions at $\sqrt{s_{NN}} = 2760$ GeV (right panel). The results are for initial parton distribution with gluon shadowing $s_g = 0.15$ (0.17) at RHIC (LHC) energies that have been fixed from the centrality dependence of $N_{\rm ch}$ data. In $p+p$ collisions, the p_T spectra from the model exhibit the LO pQCD based power law behavior at $p_T > 5$ GeV/c which is in overall good agreement with the STAR data [10]. At $\sqrt{s_{NN}} = 2.76$ TeV, we however find the calculated yield from $p+p$ overpredicts at $p_T \gtrsim 6$ GeV/c that obtained by ALICE [17] from interpolation of $p\bar{p}$ spectrum measurements at $\sqrt{s_{NN}} = 0.9$ and 7 TeV to estimate the suppression R_{AA}. For peripheral heavy ion collisions the AMPT spectra are consistent with that measured at both RHIC and LHC energies. On the other hand, the p_T distributions for central collision show marked deviation from power law function and are clearly suppressed especially at moderate $p_T = 4-11$ GeV/c due to medium modification. Though the AMPT spectra from central collisions describes the RHIC data quite well, it is however much softer than the ALICE data at $p_T > 2$ GeV/c. This possibly stems from enhanced energy loss of partons in a much denser medium that is generated from melting of strings to their valence quarks and antiquarks in the QGP medium.

The nuclear modification factor R_{AA} for charged hadrons is shown in Fig. 5 for central and peripheral Au+Au collision at RHIC (top panel) and in Pb+Pb collisions at LHC (bottom panel). For central collisions at both energies, $R_{AA}(p_T)$ is less than unity which implies appreciable suppression of charged hadrons relative to NN reference. The model calculations, with nuclear shadowing parameter $s_g = 0.15$ constrained from $dN_{\rm ch}/d\eta$ data in Au+Au collisions, describes the magnitude and pattern of the RHIC suppression data [10]. It is seen that R_{AA} increases gradually with p_T reaches a maximum of $R_{AA} \simeq 0.7$ at $p_T \simeq 1.8$ GeV/c, then it decreases with further increase of p_T and saturates thereafter to about 0.2 at $p_T \gtrsim 7$ GeV/c. The success of AMPT at $\sqrt{s_{NN}} = 0.2$ TeV thus suggests that the initial state shadowing of pQCD jet spectra, the final state scattering and the parton energy loss is consistent with the formation and evolution of the medium at RHIC energy.

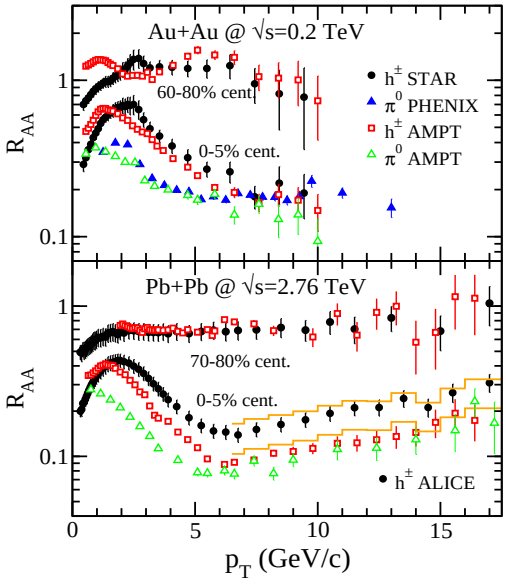

FIG. 5: Nuclear modification factor R_{AA} for charged hadrons and neutral pions as a function of p_T in central and peripheral Au+Au collisions at $\sqrt{s_{NN}} = 0.2$ TeV (top panel) and Pb+Pb collisions at $\sqrt{s_{NN}} = 2.76$ TeV (bottom panel). The AMPT model predictions are compared to the data from STAR [10] and PHENIX [11] at RHIC and from ALICE [17] at LHC. The histograms is the systematic error band due to different interpolation procedure used in earlier estimates by ALICE for the baseline $p+p$ spectra.

At $70-80\%$ centrality Pb+Pb collisions at $\sqrt{s_{NN}} = 2.76$ TeV, the R_{AA} for charged hadrons is nearly constant at about 0.7 over a large p_T range as seen in both the ALICE data [17] and AMPT model calculations. At this peripheral collision, the QGP even if formed, should have a small volume and short lifetime. In central Pb+Pb collisions at LHC, the rise and fall pattern exhibited by R_{AA} up to $p_T \sim 6$ GeV/c is similar to RHIC. However, as evident from ALICE data, the suppression of

charged hadrons at low p_T is somewhat larger, and R_{AA} reaches a minimum of 0.14 around 6-7 GeV/c. The earlier estimates with large errors as shown by histogram is due to interpolation procedure used by ALICE to obtain the baseline $p+p$ spectrum. With the recently measured spectrum in $p+p$ collision at $\sqrt{s_{NN}} = 2.76$ TeV [6], the measured R_{AA} drops but remains well within the systematic error bands which is also consistent with the CMS data [18]. In contrast to ALICE data, the AMPT calculations show even more pronounced suppression at $p_T > 2$ GeV/c due to significant quenching of the hard-scattered partons. Within the coalescence mechanism for hadronization in AMPT, though the peak positions and the subsequent decreasing pattern of R_{AA} are similar to the measured RHIC and LHC data, the minimum is found to be at 0.09 at $p_T \sim 6$ GeV/c. The subsequent rise of R_{AA} (compared to nearly constant value at RHIC) essentially stems from harder unquenched pQCD jet spectra at LHC and found to have similar slope as in the data. The significant suppression in AMPT much below than the ALICE data suggests that the medium with more than a factor of two larger parton density than RHIC is in fact more transparent than expected. Attempts to increase R_{AA} at high p_T by decreasing the shadowing s_g or by reducing the jet-medium coupling from the value $\alpha_s = 0.3$ used at both RHIC and LHC only result in an enhanced bulk (soft) hadron production and thus disagree with the centrality dependence of $dN_{\rm ch}/d\eta$ data shown in Fig. 3. In fact, the WDGH jet energy loss model [31] that has been constrained to fit the RHIC suppression data severely underpredicts the central R_{AA} value of ALICE. This posses a serious theoretical challenge to understand the underlying energy loss mechanism at the LHC energy regime.

In Fig. 5 we also show the R_{AA} for neutral pions for central collisions. As seen in charged hadrons, the R_{AA} for π^0 exhibit a similar but a gradual rise and fall pattern at intermediate p_T ($1.8 < p_T < 5$ GeV/c) and thereafter saturates (rises) with increasing p_T at RHIC (LHC) energies. Both the calculation and PHENIX data show that relative to charged hadrons, the π^0s are more suppressed by as much as $\sim 45\%$ at the intermediate p_T. However, at $p_T \gtrsim 5$ GeV/c the magnitude of suppression are nearly same for neutral pion and charged hadrons. The larger R_{AA} for charged hadrons compared to neutral pions can be explained as due to large baryonic (protons and antiprotons) yield produced from parton coalescence used for hadronization [32, 33]. In fact we find the invariant yield of pions and protons become comparable at $p_T \sim 2-4$ GeV/c. At $p_T \gtrsim 6$ GeV/c, as pions are the most abundant particles and moreover the parton spectra become gradually flatter with increasing p_T, coalescence of hard partons is seen in AMPT to predict in nearly identical suppression R_{AA} for pions and hadrons.

4. Summary and conclusions

In summary, we study the nuclear medium effects on hadron production over a wide range of p_T in Pb+Pb collisions at the LHC energy $\sqrt{s_{NN}} = 2076$ GeV. For this purpose we use the AMPT model which is updated to include the HIJING 2.0 version for initial conditions for parton distribution. We find final-state parton scatterings reduce significantly the hadron multiplicity at midrapidity that enforces smaller gluon shadowing for agreement with the ALICE data for charge particle yield at various centralities. With such a constrained parton shadowing, we find that parton energy loss in AMPT describes quite well the magnitude and suppression pattern of hadrons in both central and peripheral Au+Au collisions at the RHIC energy $\sqrt{s_{NN}} = 200$ GeV. Relative to ALICE data at LHC, the model however predicts larger jet quenching for central collision. This poses serious theoretical challenges to understand the unexpected less opaque strongly coupled plasma formed at the LHC energy.

References

[1] M. Gyulassy and L. McLerran, Nucl. Phys. A 750 (2005) 30;

E.V. Shuryak, Nucl. Phys. A 750 (2005) 64.
[2] I. Arsene et. al., Nucl. Phys. A 757 (2005) 1.
[3] B.B. Back et. al., Nucl. Phys. A 757 (2005) 28.
[4] J. Adams et. al., Nucl. Phys. A 757 (2005) 102.
[5] K. Adcox et. al., Nucl. Phys. A 757 (2005) 184.
[6] J. Schukraft for the ALICE Collaboration, arXiv:1106.5620.
[7] B. Wyslouch for the CMS Collaboration, arXiv:1107.2895.
[8] P. Romatschke and U. Romatschke, Phys. Rev. Lett. 99 (2007) 172301.
[9] H. Song and U. Heinz, Phys. Lett. B 658 (2008) 279.
[10] J. Adams et. al., Phys. Rev. Lett. 91 (2003) 172302.
[11] S.S. Adler et. al., Phys. Rev. C 69 (2004) 034910.
[12] M. Gyulassy, P. Levai, and I. Vitev, Phys. Rev. Lett. 85 (2000) 5535.
[13] M. Gyulassy, I. Vitev, X.N. Wang, and B.W. Zhang, in *Quark Gluon Plasma*, ed. by R.C. Hwa and X.N. Wang (World Scientific, Singapore, 2004); A. Kovner and U.A. Wiedemann in *Quark Gluon Plasma*, ed. by R.C. Hwa and X.N. Wang (World Scientific, Singapore, 2004).
[14] S. Pal and S. Pratt, Phys. Lett. B 574 (2003) 21; S. Pal Phys. Rev. C 80 (2009) 041901(R).
[15] K. Aamodt et. al., Phys. Rev. Lett. 106 (2011) 032301.
[16] CMS Collaboration, arXiv:1107.4800.
[17] K. Aamodt et. al., Phys. Lett. B 696 (2011) 30.
[18] A.S. Yoon for CMS Collaboration, arXiv:1107.1862.
[19] X.-F. Chen, T. Hirano, E. Wang, X.-N. Wang, and H. Zhang, arXiv:1102.5614.
[20] S. Scherer et al. Prog. Part. Nucl. Phys. 42 (1999) 279.
[21] Z.W. Lin, C.M. Ko, B.-A. Li, B. Zhang, and S. Pal, Phys. Rev. C 72 (2005) 064901.
[22] Z. Xu and C. Greiner, Phys. Rev. C 76 (2007) 024911.
[23] W.-T. Deng, X.-N. Wang, and R. Xu, Phys. Rev. C 83 (2011) 014915; Phys. Lett. B 701 (2011) 133.
[24] S. Li and X.N. Wang, Phys. Lett. B 527 (2002) 85.
[25] X.N. Wang and M. Gyulassy, Phys. Rev. D 44 (1991) 3501.
[26] D.W. Duke and J.F. Owens, Phys. Rev. D 30 (1984) 49.
[27] M. Glück, E. Reya, and W. Vogt, Z. Phys. C 67 (1995) 433.
[28] J. Xu and C.M. Ko, Phys. Rev. C 83 (2011) 034904.
[29] I.G. Bearden, et. al., Phys. Rev. Lett. 88 (2002) 202301.
[30] S.S. Adler, et. al., Phys. Rev. C 71 (2005) 034908.
[31] W.A. Horowitz and M. Gyulassy, arXiv:1104.4958.
[32] V. Greco, C.M. Ko, and P. Levai, Phys. Rev. Lett. 90 (2003) 202302.
[33] R.J. Fries, B. Muller, C. Nonaka, and S.A. Bass, Phys. Rev. Lett. 90 (2003) 202303.